



# The most filigree structure made by remote laser cutting

Robert Baumann<sup>1,2</sup>, Patrick Herwig<sup>2</sup>, Eckhard Beyer<sup>1,2</sup>

- 1) Institut für Fertigungstechnik, Technische Universität Dresden(TUD), Georg-Bähr Straße 3C  
Dresden, Germany
- 2) Fraunhofer-Institut für Werkstoff und Strahltechnik (IWS), Winterbergstraße 28, 01277 Dresden,  
Germany

## Keywords

Open cell foam, laser, cutting, remote, aluminium

## Abstract

It is well known that the global climate change is the largest challenge for the society of the 21st century. In order for us to manage the resulting consequences, innovative materials for energy efficient applications become more and more important [1]. Open cell metal foam contributes promising solutions to the light weight design, battery applications and renewable energy harvesting [2]. Still, challenges are present concerning the cutting into a defined shape. The remote laser cutting offers a solution for decreasing the production costs as well as the needed component accuracy. Our investigations consider that this technique has a high potential concerning cutting speed which was increased by more than 500 %, compared to state of the art laser separation. Next to that, the contour accuracy was improved as well, resulting in tolerances with less than 30 µm. Together with the forceless process of remote laser cutting, the possibility is given to generate filigree components with a wall thickness less than 0.75 pore sizes. This paper offers insight into the viability of remote laser cutting in overcoming the challenges dealing with mechanical milling or grinding. Investigating the process concerning thermal stress input as well as particle attachments will be the next steps in the future.

## 1 Introduction

Innovative materials like open cell metal foams deliver promising solutions in the field of light weight design and energy efficient applications (heat exchangers, battery systems) for overcoming the imminent challenges of the global climate change. Nevertheless, those solutions need to be affordable for customers of the final component. Cost reduction is increasingly becoming a vital factor in production processes. Different opportunities had to be explored, in order to fulfil the demand for a higher rate of flexibility compared with large scale production. Traditional mechanical processes like milling or grinding were investigated to close this gap [2-5]. Nevertheless, the disadvantages such as tool costs and tool wear still limit the potential. In addition, milling modifies the surface property resulting in a smearing effect. Moreover, this concludes in a loss of the cellular structure. Current solutions to increase the production speed are unsatisfactory. Mechanical processes deliver cutting speed of 5 m/min which is not high enough for large scale production [6-7].

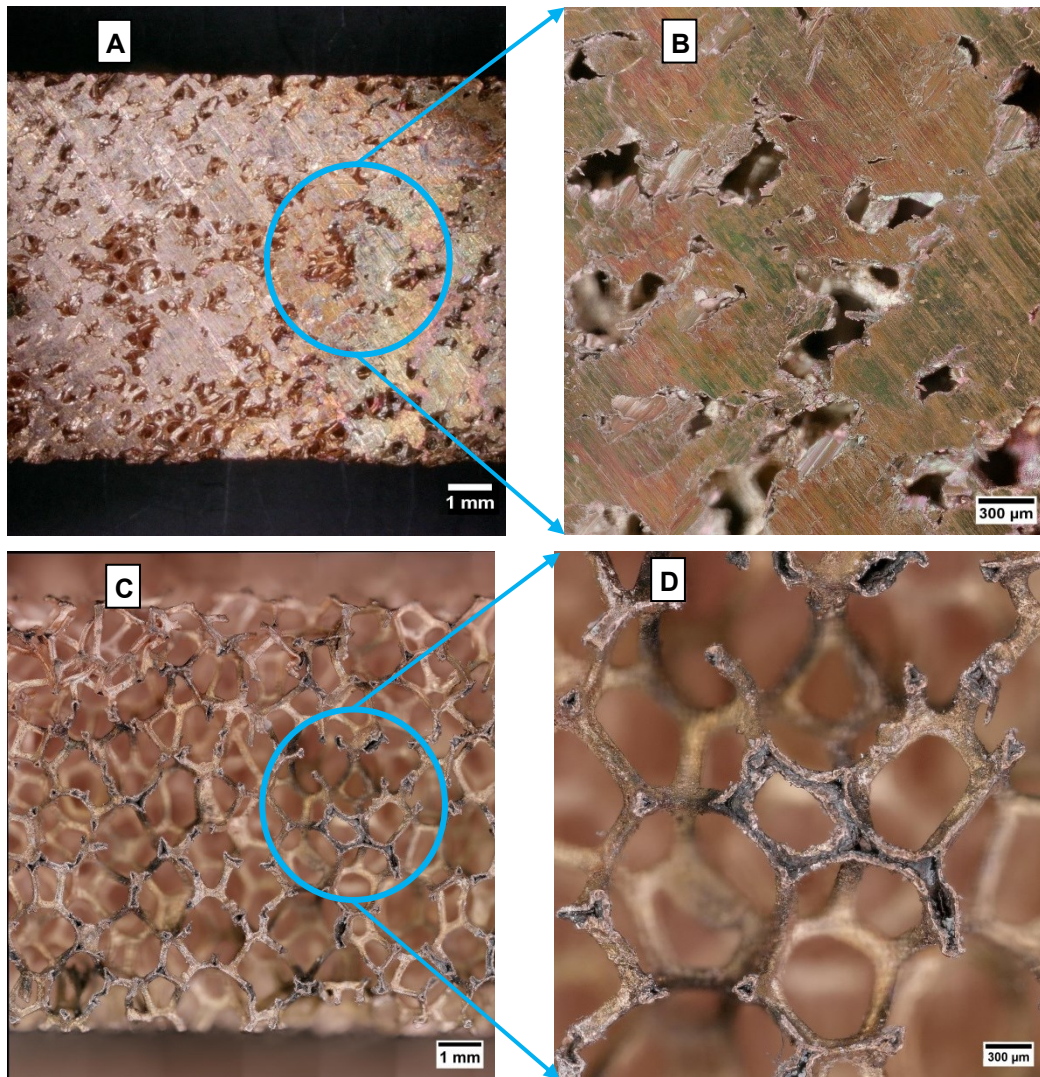


Figure 1: Microscopic investigation of the smearing effect: Overview of smeared surface (A) and microscopic image (B) of metal foam after mechanical machining; overview of untreated metal foam with open porosity (C) and magnification with a microscope (D)

In contrast, laser technology is a new approach for cutting metal foam due to the fact that it is a wear-free and highly flexible process [8]. Several experiments were carried out using the laser fusion cutting technology [9]. Furthermore, this is an established separation technique in various fields of industrial applications. The basic principle is well known as the laser beam is absorbed at the surface of the material and melts the entire bulk at once. A coaxial high pressure gas stream (for example N<sub>2</sub>, Ar, or air) ejects the molten material to the bottom side of the specimen [8]. Due to melting the entire bulk in the cut kerf at once, a thermal stress is induced. Consequently, several investigations are dealing with induced thermal stress into the foam material in order to determine and evaluate the cutting parameters as well as the geometry of the contour [9-11]. Additionally, the property of the open cell structure decreases the combustion of the process gas. Nevertheless, dross attachments as well as thermal stress are the biggest challenges that have to be investigated in more detail.

Remote cutting is a promising approach in sizing with laser. Moreover, it has the possibility to reduce the thermal induced stress. Furthermore, the open cell structure will be kept as well as the preferred contour outline. The investigation verifies the novel remote laser cutting technique for open cell foams. Relevant core themes of the research are the achievable separation velocity, edge geometry and minimal wall width.

The second section will give an introduction into the experimental setup. Explaining the basic principle of remote laser cutting as well as the methodology are the major subjects in the section. A special focus is set on the imaging process and how it can be used for getting reliable results. Consequently,

the third section focusses on the material characterization and the cutting process parameters. Finally, the fourth section illustrates the results regarding the four major core themes.

## 2 Materials and methods

Since the basic physical principle is not well known, this section will describe the remote laser cutting in more detail. The laser beam is absorbed at the surface and melts only a small volume of the irradiated area. Next to the molten part, a certain kind of material is vaporized. This vapour is called steam cavity and consists of a high amount of pressure, which ejects the molten material. For achieving the steam cavity in the cut kerf, a high intensity of the laser beam is required. It is known that this could be achieved by using small spot sizes in the focal plane. The cut kerf is created in a gradual ablation. Moreover, the melt and vapour is ejected to the top side of the specimen. Consequently, small spot sizes ( $\varnothing_{\text{spot}} < 100 \mu\text{m}$ ) at large working distances require a high beam parameter product (BBP). Accordingly, a single mode fibre laser was utilized for the following investigations [12].

The word “remote” in the context of laser cutting describes the beam manipulation system which focuses and deflects the laser radiation. Hence, the beam gets deflected over mirrors which are attached on highly dynamic galvanometric drives. Typically, a larger distance (up to 650 mm) to the material surface is adjusted compared to other laser cutting technologies (0.5 mm – 1.5 mm). Summarizing the different separations techniques, the basic principle of the remote laser cutting and fusion cutting is illustrated in Figure 3.

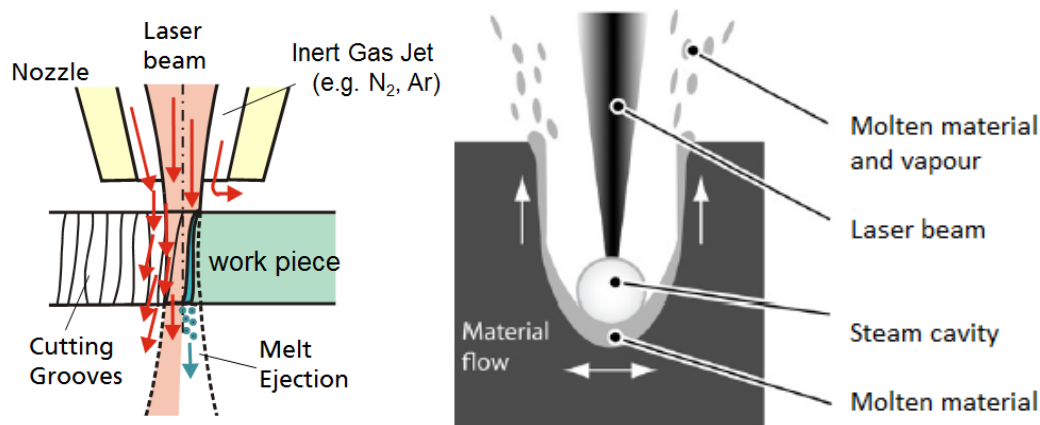


*Figure 2: Theoretical work principle of laser fusion (left) and laser remote (right) cutting [12]*

Laser remote cutting as an alternative separation technique for metal foams will be discussed in terms of four main criteria: achievable cutting speed, edge shape, thermal damaging and oxygen distribution. Due to the fact that the laser beam is deflected by mirrors, cutting speeds of up to 1200 m/min are possible. Furthermore, stepwise ablation of the material during remote cutting offers an opportunity to manipulate specific process parameter (idle time between cycles, cross jet pressure, scan velocity). Moreover, optimizing these can reduce the thermal damage zone.

As mentioned, for the remote laser cutting technique high brilliant beam sources are indispensable. For the following investigations, a single mode fibre laser with a maximum output power of 5000 W is utilized. Due to the fact that the beam size has a significant influence to the spot size, a collimator with a focal length of 200 mm is used [13]. As a beam manipulation system a scanner with an aperture of 20 mm and a focal lens (500 mm focal length) was considered. The results of the optical components are measured with a laser beam diagnostic system and shows spot values of 86  $\mu\text{m}$ .

In this report, open cell foam out of steel-316L and aluminium were investigated. Table 1 present the most important material parameters.



Table 1: Material and properties

Material	Thickness [mm]	Pore size [ $\mu\text{m}$ ]
steel	1.6	450
steel	1.9	580
steel	2.7	800
steel	3.2	1200
aluminium	5.5	2000
aluminium	10	1800

For determining the possible cutting speed, the results had to be categorized into three different groups. All samples were analysed via microscopy and defined as “cut”, “nearly cut” and “no cut”. A sample, which is located in the “cut” category possess a complete and clear kerf without any struts, as illustrated in Figure 3 left. While a “nearly cut” offers some remaining and a “no cut” shows multiple incomplete sections in the kerf (Figure 3). Moreover, with this cut categorization the possibility to determine the cutting velocity for both setups and foams is given.

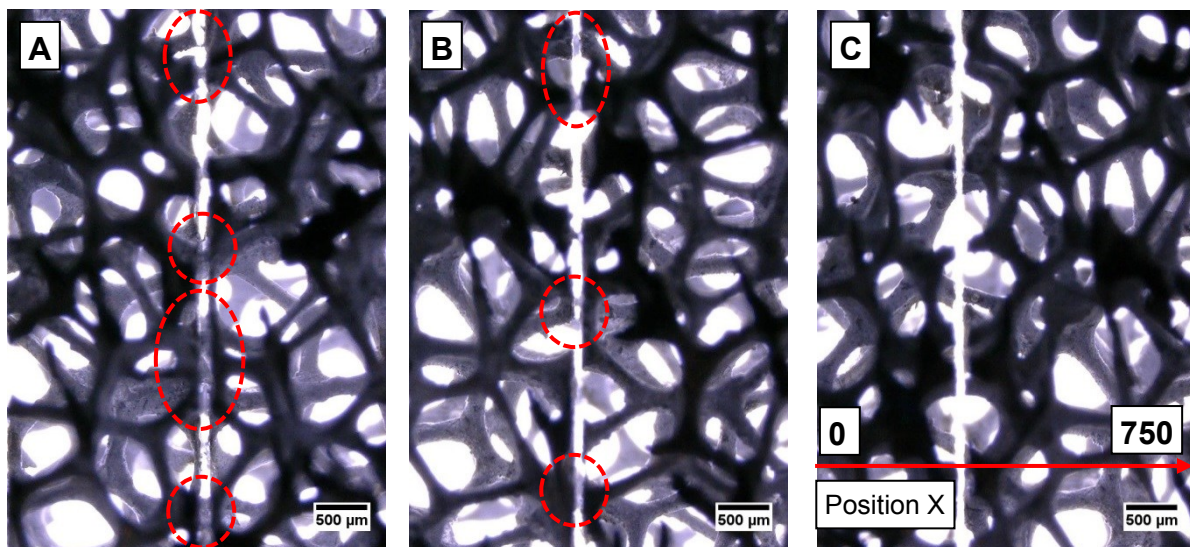


Figure 3: Optical analysed samples and classification into the different cut categories, “no cut” is displayed on the right, “nearly cut” is illustrated in the middle and “cut” is presented in the left image

First of all, an image of the surface as in Figure 3 of the sample was taken and segmented into vertical lines. Consequently, the background of the images was white, which represents a grey value of 255. The average grey value of these vertical lines ( $0 < I_{gv} < 255$ ) were calculated and recorded. If a grey value is above the 250, the sample was set into the “cut” category. A grey value between 230 and 250 represents the “nearly cut”. All remaining results can be seen as a “no cut”. This process is exhibit in Figure 4.

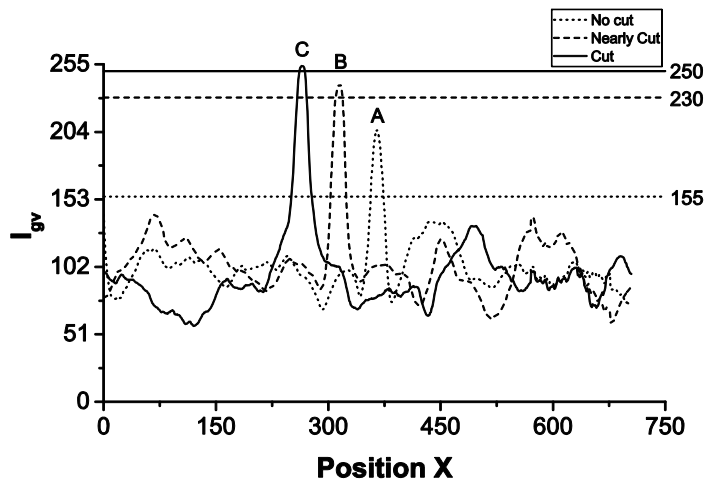


Figure 4: Classification into different cut categories

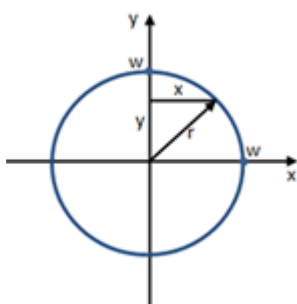
Next to the determination into the three different categories, a similar imaging process was executed in order to measure the impact of cut process parameters to the cutting depth. Note that the distribution of the data points is large for open cell metal foam due to the build-up structure. For overcoming this challenge, ten images were taken of laser unaffected foam to determine the threshold, which can be seen as a reference. A complete cut will be seen as a grey value above 250. In order to evaluate the cut depth, the average out of four images for one depth value was considered. Note that it is nearly impossible to measure the correct cut depth due to the foam structure, but this can be seen as a close approximation of the value. Therefore, the impact of the parameters on the cutting result (cut velocity) can be estimated.

Concerning the determination of tolerance, all data were taken by standardized and gauged measuring machine. This machine has the opportunity to gather the data ductile and optical. In this case the measurements were taken with an optical tool.

$$F := I \cdot t \rightarrow \text{Fluence of radiation} \quad (1)$$

F ... fluence  
I ... intensity  
T ... interaction time

The beam shows a Gaussian intensity distribution:



$$I(r) = I_0 \cdot e^{-2\left(\frac{r}{w}\right)^2} = \frac{2 \cdot P}{\pi \cdot w^2} \cdot e^{-2\left(\frac{r}{w}\right)^2} \quad (2)$$

$$I(x, y) = I_0 \cdot e^{-2\left(\frac{x}{w}\right)^2} \cdot e^{-2\left(\frac{y}{w}\right)^2} \quad (3)$$

$$E = \iint_{-\infty}^{\infty} F(x, y) dx dy \quad (4)$$

$$F(x, y) = I_0 \cdot \int_{-\infty}^{\infty} e^{-2\left(\frac{x}{w}\right)^2} \cdot e^{-2\left(\frac{y}{w}\right)^2} dt \quad (5)$$

$$v = \frac{x}{t} \rightarrow x = v \cdot t \quad (6)$$

$$F(v, y) = \sqrt{\frac{2}{\pi}} \cdot \frac{P}{w \cdot v} \cdot e^{-2\left(\frac{y}{w}\right)^2} \text{ and } F_0 = \sqrt{\frac{2}{\pi}} \cdot \frac{P}{w \cdot v} \quad (7)$$

P ... laser power

v ... velocity of laser beam at the surface

w ... radius laser beam

A beam with a fluence distribution  $F(r)$  moves with a constant velocity  $v$  in  $x$ -direction. If the maximum fluence  $F_0$  is larger than the effect threshold  $F_{th}$  the materials changing appears in strips as shown in Figure 5.

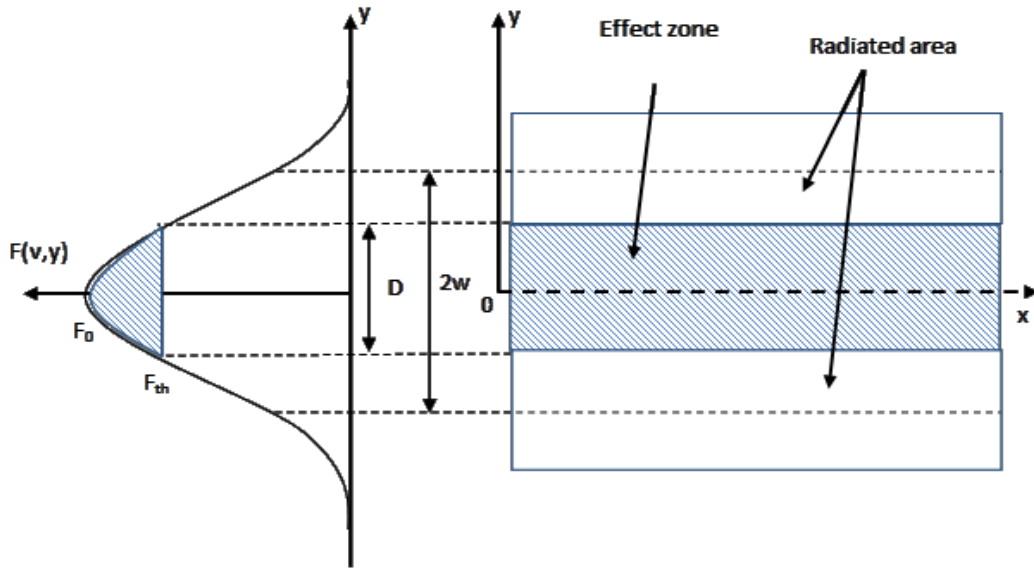


Figure 5: Fluence distribution of a moved laser beam and resulting effect zone width at the material surface fluence distribution of a moved laser beam and resulting effect zone width at the material surface

The width of the effect zone is  $D$ . In this section the maximum Fluence  $F_0$  exceeds the effect threshold  $F_{th}$  for a moved laser beam. Moreover, the width  $D$  depicts a fluence distribution  $F(v,y)$  at  $F(v, D/2) = F_{th}$ . Hence,  $D$  can be calculated with the equation 7.

$$F(v,y) = F_0 \cdot e^{-2\left(\frac{y}{w}\right)^2} \text{ with } F_0 = \sqrt{\frac{2}{\pi}} \cdot \frac{P}{w \cdot v} \quad (8)$$

$$\ln\left(\frac{F(v,y)}{F_0}\right) = -2\left(\frac{y}{w}\right)^2 \quad (9)$$

$$y^2 = \frac{w^2}{2} \cdot \ln\left(\frac{F_0}{F_{th}}\right) \quad (10)$$

At  $F(v,y) = F_{th}$  should  $y = D/2$  (see Figure 5), which concludes in:

$$D^2 = 2 \cdot w^2 \cdot \ln\left(\frac{F_0}{F_{th}}\right) \quad (11)$$

### 3 Results

For determining the cutting speed, the maximum fluence  $\ln F_0$  was linearly raised over increasing the laser power and the numbers of scan cycles were adapted to achieve a complete cut, respectively. Moreover, the scan velocity was set constant at 10 m/s. In conclusion, a correlation between cut velocity and maximum fluence  $F_0$  is illustrated in Figure 6.

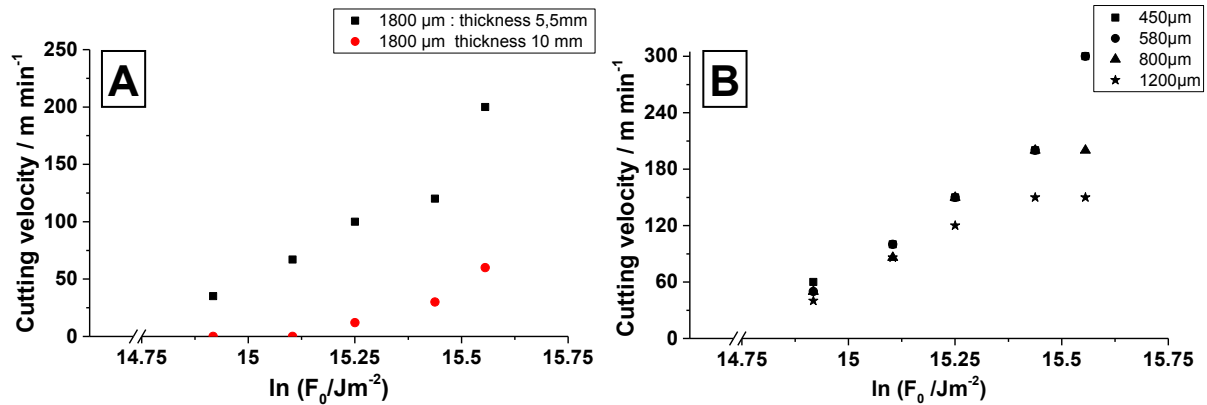
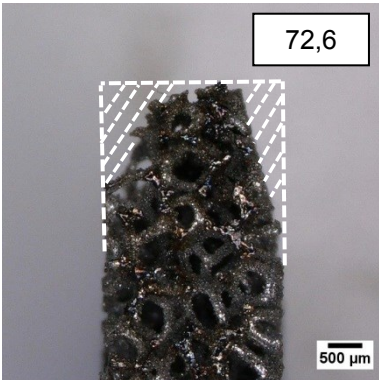
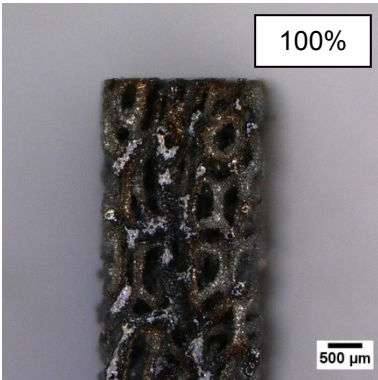
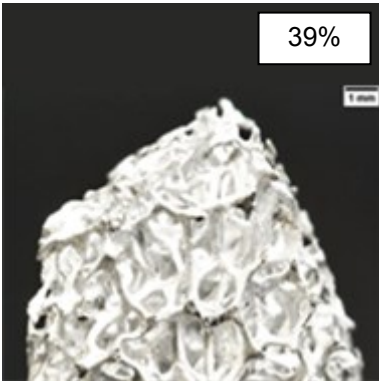
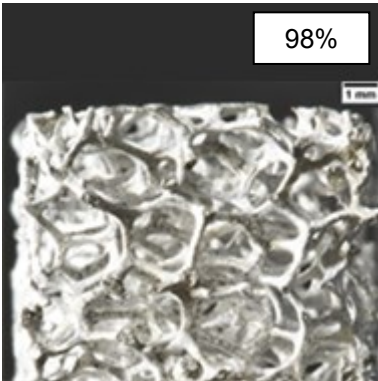


Figure 6: Achievable cut velocity depending on the max. fluence for aluminium (A) and steel (B) foam

The setup indicates for the investigated material thicknesses a nearly linear rising of the achievable cutting speed as demonstrated in Figure 6. With higher fluence, more cell struts are cut in one cycle. Therefore, a complete cut is achieved with fewer cycles, which leads to higher cutting speed. Lower intensities demand more cycles, which lead to an unfavourable heat up of the cutting edge. Note that for steel foam the largest pore size always has the slowest cutting speed. The material thickness and the stepwise cutting process, which was described earlier, cause this effect. Compared to the state of the art, high rates of cut velocities could be achieved [6-7]. Additionally, it can be seen that the maximum cut velocity is 300 m/min for various pore sizes. Previous investigations depict a similar cutting speed for various materials and pore sizes [14-16]. This is caused by the maximum possible scan velocity of the utilized scanner. On the one hand, the size of the scan mirrors defines the dynamic behaviour; on the other hand, it limits the possible utilized laser power. Smaller mirrors possess a higher dynamic behaviour. Consequently, a lower fluence is mandatory due to the less allowed laser power.

A geometrical feature of the cut area has to be investigated as well. As mentioned, state of the art separation techniques like grinding, milling or punching are creating a disorientation of the edge. Especially punching influences the edge geometry due to a clutching effect. Exemplarily, the determination of the degree of utilization is depicted in Table 2.

Table 2: Determination of the degree of utilization for steel and aluminium foam

Material / Pore size	Mechanical cut	Laser cut
Steel 316L / 1200 $\mu\text{m}$		
Aluminium / 1800 $\mu\text{m}$		

As demonstrated in Table 2, the hatched area represents the amount of material which is lost. In conclusion, only 72.6 % of the material at the edge is operative for the designed purpose. Note that the material is getting squeezed into the remaining foam structure which influences the pore size and distribution. In comparison, laser cutting shows no edge deformation or squeezing. For all different pore sizes the remaining material at the edge was calculated and illustrated in Table 4. It shows that the degree of utilization for remote laser separated foam is mostly at 100 %, whereas the mechanical cut creates values between 82 % and 39 %. This 100 % degree of utilization could be explained by the forceless separation with laser beams. It is well known that with increasing pore size the material thickness is getting larger due to fabrication aspects [4]. A larger pore size and foam thickness lead to a greater area which is affected by the cutting force. That is why an increase of the pore size leads to a decrease of the degree of utilization.

Table 3: Achievable degree of utilization

Material	Thickness	Pore size	Mechanical cut	Laser cut
steel	1.5 mm	450 $\mu\text{m}$	82.1 %	100 %
steel	1.8 mm	580 $\mu\text{m}$	73.3 %	100 %
steel	2.3 mm	800 $\mu\text{m}$	73.4 %	100 %
steel	3.2 mm	1200 $\mu\text{m}$	72.6 %	100 %
aluminium	5.5 mm	1800 $\mu\text{m}$	60.1 %	100 %
aluminium	10.0 mm	1800 $\mu\text{m}$	39 %	98 %

For determining the achievable contour accuracy, a round blank specimen was cut with a programmed diameter of 15 mm. A cut kerf correction was not executed, which leads to a smaller measured diameter of the circle. For each porosity and their correspond thickness, ten circles were



manufactured. Each measured circle consists of 20,000 data points. In Table 4 the results are illustrated.

*Table 4: Achievable accuracy for steel foam depending on the pore size*

Pore size	450 $\mu\text{m}$	580 $\mu\text{m}$	800 $\mu\text{m}$	1200 $\mu\text{m}$
Accuracy	$\pm 22.5 \mu\text{m}$	$\pm 23.3 \mu\text{m}$	$\pm 30.0 \mu\text{m}$	$\pm 25.9 \mu\text{m}$

The standard deviation of the samples is important because it represents the achievable tolerance. As it can be seen, component accuracies from  $\pm 20 \mu\text{m}$  to  $\pm 30 \mu\text{m}$  are possible.

Given the opportunity to separate the foam without force, the idea of slicing it into very thin parts was created. Therefore, several investigations concerning the wall thicknesses were done in order to expand the limit to the minimal achievable wall width. For the experiments, open cell metal foam out of aluminium (Pore size 2,000  $\mu\text{m}$ , thickness 5.5 mm) and steel foam (pore size 450  $\mu\text{m}$ , thickness 1.5 mm) were investigated. The results are illustrated in Figure 6.

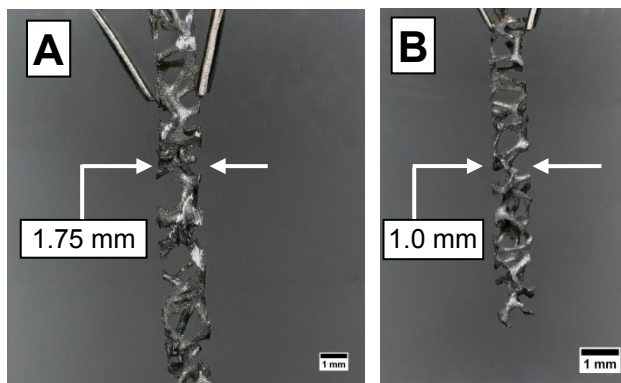


*Figure 6: Achievable wall thickness with remote laser cutting of aluminium foam 2000  $\mu\text{m}$  pore size (A, B)*

As it can be seen in Figure , the wall thickness for steel foam is 400  $\mu\text{m}$ . This is less than one pore size. For open cell metal foam out of aluminium the minimal achievable wall width was 1.0 mm. It is well known that the connections between the single pores maintain the structural integrity of the sample. Thinner components are possible but with decreasing wall width the possibility that no connections between the pores remain is given. Consequently, samples with thinner walls can be cut but this would be an unsecure production process. Our investigations lead to the conclusion that it takes multiple trials in order to achieve components with less than 0.5 pore sizes as a wall thickness. Nevertheless, it is possible to produce a foam structure with less than 0.25 pore sizes, illustrated in Figure 7.

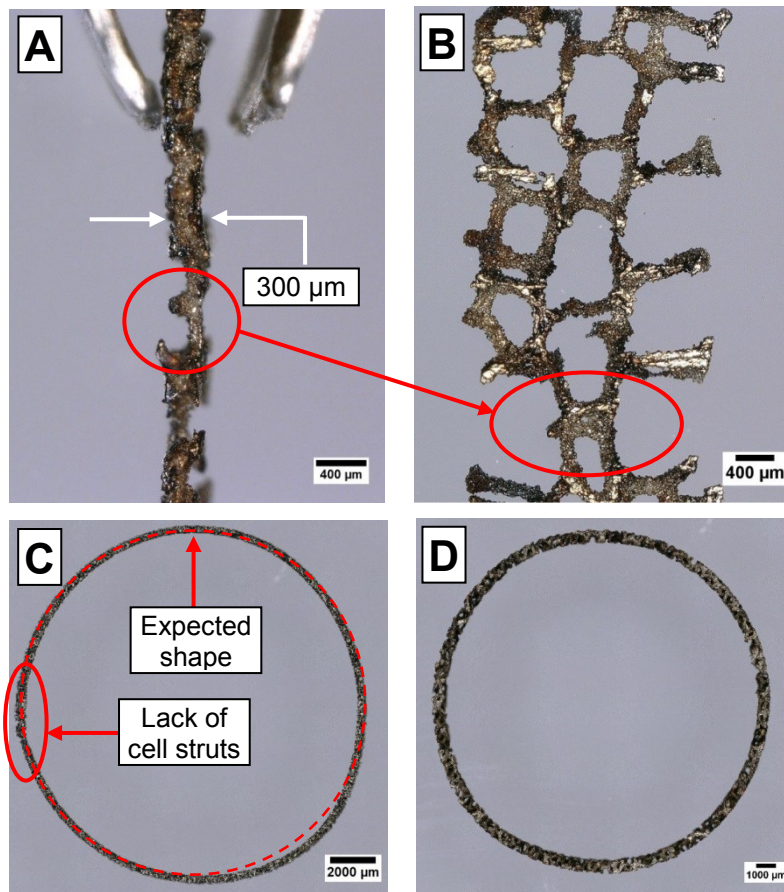


Figure 7: Microscopic Images of steel foam, pore size 1200  $\mu\text{m}$ ; top view of the cutting edge (A), side view at the foam structure (B), top view on laser remote cut steel foam with a pore size of 450  $\mu\text{m}$  (C), top view on steel foam with a pore size of 1200  $\mu\text{m}$  (D)

As demonstrated in Figure 7, parts of foam structure depict only one or two struts in the cross section. This creates a brittle behaviour leading to a lost in structural integrity. Due to the probability, the location of the cut edge has a huge impact on the cut result. Moreover, it has to be ensured that sufficient amount of cell struts remain in the component structure. Figure 7 (C) shows that not enough struts are present. Hence, the circle shape is not durable and process reliability is not given.

#### 4 Discussion and conclusion

In conclusion, the minimal achievable wall thickness of a component is limited to the probability of the foam structure. For our investigation, we recommend a minimal wall thickness of 0.6 pore sizes in order to achieve a reliable process. In summary, the remote laser cutting offers solutions for upcoming challenges concerning the shaping of open cell metal foam. An achievable cutting speed from up to 300 m/min is possible for open cell steel foam. Note that with larger pore size the material thickness increased respectively, which concludes in a lower separation velocity. In addition to the cutting speeds, the results shows the correlation between fluence and size of the thermal effect zone. Tolerances from less than  $\pm 30 \mu\text{m}$ , for some pore sizes  $\pm 20 \mu\text{m}$ , are attainable. A major leap forward was made concerning slicing the foam into thin components. Wall width with less than one pore size is achievable for several materials and porosities. Further investigations will consider an increase of material thickness as well as different materials such as Nickel and several alloys.

## References

- [1] Umweltbundesamt (Hrsg): Treibhausgasneutrales Deutschland im Jahr 2050. Studie. Dessau-Roßlau, 01.10.2013, zuletzt geprüft am 16.09.2015.
- [2] Ashby, M. F.; Evans, A. G.; Fleck, N. A.; Gibson, L. J.; Hutchinson, J. W.; Wadley, H. N.G.: *Metal Foams: A Design Guide*. Butterworth-Heinemann: Elsevier, 2000.
- [3] Banhart, J.: Eigenschaften und Anwendungsgebiete offenporiger metallischer Werkstoffe. *Aluminium*, 12 (1999), pp. 1094–1099.
- [4] Bram, M.; Kempmann, C.; Laptev, A.; Stöver, D.; Weinert, K.: Investigations on the Machining of Sintered Titanium Foams Utilizing Face Milling and Peripheral Grinding. *Adv. Eng. Mater.*, 5(6) (2003), pp. 441–447. doi: 10.1002/adem.200300356
- [5] Vogt, M.; Malanoski, N.; Glitz, R.; Stahl-Rolf, S: *Bestandsaufnahme Leichtbau in Deutschland*. VDI, Berlin, 2015.
- [6] Weinert, K.; Bram, M.; Kempmann, C.; Stöver, D.: Machinability investigations concerning the milling and grinding of metal foams. *Prod. Eng.*, 10(2) (2003), pp. 65–70.
- [7] Hunt, C.: A method to reduce smearing in the milling of metal foams, Iowa: Iowa State University, 2009.
- [8] Hügel, H.; Graf, T.: *Laser in der Fertigung*. Wiesbaden: Vieweg + Teubner, 2009.
- [9] Yilbas, B. S.; Akhtar, S. S.; Keles, O.: Laser cutting of small diameter hole in aluminum foam. *Int. J. Adv. Manuf. Technol.*, 79(1–4) (2015), pp. 101–111. doi: 10.1007/s00170-015-6789-8
- [10] Yilbas, B. S.; Akhtar, S. S.; Keles, O.: Laser cutting of triangular geometries in aluminum foam: Effect of cut size on thermal stress levels. *Opt. & Laser Technol.*, 48 (2013), pp. 523–529. doi: 10.1016/j.optlastec.2012.11.026
- [11] Yilbas, B. S.; Akhtar, S. S.; Keles, O.: Laser hole cutting in aluminum foam: Influence of hole diameter on thermal stress. *Opt. & Laser Technol.*, 51(1) (2013), pp. 23–29. doi: 10.1016/j.optlaseng.2012.08.002
- [12] Lütke, M.: *Entwicklung des Remote-Laserstrahlschneidens metallischer Werkstoffe*. TU Dresden, Diss., 2011.
- [13] Eichler, J.; Eichler, H.: *Laser - Bauformen, Strahlführung, Anwendungen*. Berlin: Springer, 2006.
- [14] Baumann, R.; Herwig, P.; Wetzig, A.; Beyer, E.: Precise laser separation of hollow metallic copper structures. In: *Metfoam 2015 – 9th International Conference on Porous Metals and Metallic Foams*, Barcelona, August 31st–September 2nd 2015.
- [15] Baumann, R.; Herwig, P.; Wetzig, A.; Beyer, E.: Swift and accurate – investigation of remote laser cutting for open cell foams. In: *LiM 2017 - 9th International WLT Conference on Lasers in Manufacturing*, München, 26–29 June 2017.
- [16] Baumann, R.; Herwig, P.; Wetzig, A.; Beyer, E.: Investigations of Corrosion Resistance of Laser Separated Open Cell Metal. *Adv. Eng. Mater.*, 19(10) (2017). doi: 10.1002/adem.201700107